Chinese Chemical Letters 32 (2021) 761–764

Contents lists available at ScienceDirect

Chinese Chemical Letters

journal homepage: www.elsevier.com/locate/cclet

Communication

The relationship of morphology and catalytic performance of CeO_2 catalysts for reducing nitrobenzene to azoxybenzene under the base-free condition

Xueke Zhou[1], Haitao Zhao[1], Shaojun Liu, Yang Yang, Ruiyang Qu, Chenghang Zhen, Xiang Gao*

State Key Lab of Clean Energy Utilization, State Environmental Protection Engineering Center for Coal-Fired Air Pollution Control, Zhejiang University, Hangzhou 310027, China

ARTICLE INFO

Article history:
Received 26 March 2020
Received in revised form 6 May 2020
Accepted 18 May 2020
Available online 2 June 2020

Keywords:
Ceria catalyst
Ce^{3+}proportion
Nitrobenzene
Azoxybenzene
Base-free

ABSTRACT

CeO_2 morphology was proposed to be a crucial factor for reducing nitrobenzene to azoxybenzene under the base-free condition. Herein, the structure-activity relationship of CeO_2 catalysts was explored to improve the azoxybenzene yield. A series of CeO_2 catalysts were synthesized with seven morphologies to obtain different Ce^{3+} proportion and various surface areas. Notably, the catalytic performance of these samples for reducing nitrobenzene to azoxybenzene enhanced with the increasing Ce^{3+} proportion. With the highest surface Ce^{3+} proportion, the Rod-CeO_2 catalyst exhibited 100% conversion of nitrobenzene and 89.8% azoxybenzene selectivity in 7 h at 150 °C under 1 MPa CO. Moreover, the preliminary mechanistic analysis indicated that the inhabitation of azoxybenzene to by-product azobenzene resulted in the high selectivity of azoxybenzene.

Azoxybenzene is a high-value compound with wide applications in chemical industries as dyes, pigments and agrochemicals [1,2]. Azoxybenzene is commonly obtained by oxidation of aniline or reduction of nitrobenzene as an intermediate [3,4]. The conventional production of azoxybenzene entails condensation of stoichiometric nitrosobenzene and hydroxylamine [5]. This process lacks of atom-economy and produces by-products which cause pollution troubles. To simply the reaction steps and prevent the production of hazardous by-products, the development of controlling the selectivity in the midst of nitrobenzene reduction to produce azoxybenzene is of ongoing research interest.

Recently, there are some developments reported to achieve satisfying yields of azoxybenzene in the presence of bases such as hydrazine hydrate or NaOH by transferring the reduction route of intermediate formed from nitrobenzene hydrogenation [6–8]. However, the green synthesis of azoxybenzene under the base-free condition is still a challenge. Another interesting finding is that azoxybenzene could be produced under the base-free condition catalyzed by Ni@C + CeO_2 [9]. In this research, the combination of Ni@C and CeO_2 exhibited the best catalytic performance to synthesize azoxybenzene compared with combinations of Ni@C with metal oxides such as Al_2O_3, TiO_2, SiO_2, which indicated that CeO_2 was crucial for the high yield of azoxybenzene. However, the structure-activity relationship of CeO_2 catalysts remain to be explored. For CeO_2 based catalysts, the cyclic alternation between Ce^{3+} and Ce^{4+} and the oxygen storage capacity (OSC) are regarded as the key ingredients in reactions such as hydrogenation [10], HgO oxidation [11], hydrogen generation [12], CO oxidation [13,14] and so on. As shown in the report of azobenzene synthesis by reducing nitrobenzene, the BET surface areas of Au/CeO_2 catalysts, which were related to the oxygen storage capacity, exhibited a correlation with the catalytic activities of reducing azoxybenzene to azobenzene [15]. However, the key effect factor for reducing nitrobenzene to azoxybenzene catalyzed by CeO_2 based catalysts has not been proposed.

Considering that the morphology engineering of CeO_2 is of great importance to control their surface chemistry [16–18], herein, we synthesized a series of CeO_2 samples with seven morphologies and applied them in reducing nitrobenzene to azoxybenzene. The relationship of physico-chemical properties of the seven CeO_2 catalysts and their catalytic performance was explored to improve azoxybenzene yield under the base-free condition.

In this work, the Rod-CeO_2, B-Cube-CeO_2 and S-Cube-CeO_2 samples were prepared via hydrothermal methods. Particle-CeO_2 was synthesized by precipitation method. Meso-CeO_2 was

* Corresponding author.
E-mail address: xgao1@zju.edu.cn (X. Gao).
[1] The two authors contributed equally to this work.

https://doi.org/10.1016/j.cclet.2020.05.023

prepared by hard-templating approach using KIT-6 as the hard template. Moreover, L-Particle-CeO_2 was prepared by calcination of $Ce(NO_3)_3{\cdot}6H_2O$. The detailed synthesis conditions of above catalysts are listed in Supporting information. Commercial-CeO_2 (Sinopharm Chemical Reagent Co., Ltd., 11.82 m^2/g) was purchased and used for comparison. In a typical procedure, 0.5 mmol nitrobenzene, 5 mL anhydrous toluene and a certain amount of catalysts were added in a 25 mL Parr autoclave equipped with the mechanical agitation. The autoclave was purged by N_2 for several times and sealed with 1 MPa pressure CO, followed by stirring at 1000 rpm at 150 °C. The products were separated by centrifugation and confirmed by Agilent 7890B-5977A GC-MS. The conversion and selectivity were determined with oxylene as an internal standard.

To probe the morphological characteristics of the seven CeO_2 samples, scanning electron microscope (SEM) and transmission electron microscopy (TEM) were carried out and shown in Fig. 1. According to the images observed in Figs. 1a and b, Rod-CeO_2 exhibits a width of 9–18 nm and a length of 70–320 nm. Figs. 1c–f depict that L-Particle-CeO_2 and Particle-CeO_2 are irregular particles with diameters of 5–20 nm and 5–18 nm respectively, while L-Particle-CeO_2 is longer than Particle-CeO_2 observed in TEM images. Synthesized by the hard-templating approach with mesoporous silica as templates, the images shown in Figs. 1g and h demonstrate that the well-ordered structures and mesoporous channels of Meso-CeO_2 samples were corresponding to the replicated KIT-6. From Figs. 1i–l, S-Cube-CeO_2 and B-Cube-CeO_2 show regular cubic shapes with varying size distributions of 7–32 nm and 16–140 nm respectively. Used for comparison, Commercial-CeO_2 samples shown in Figs. S1a and b (Supporting information) present irregular configuration with diameters between 7 nm and 42 nm.

To obtain the crystal sizes and identify the crystal phases, X-ray diffraction (XRD) was carried out with the results presented in Fig. S2 (Supporting information). All the diffraction peaks could be indexed to the typical fluorite structure of pure CeO_2. Related to the crystallinity, the width of the peaks can be used to estimate the mean crystallite size of CeO_2 based on the Scherrer's equation. From Table 1, the mean crystallite sizes follow the order B-Cube-CeO_2 > Commercial-CeO_2 > S-Cube-CeO_2 > Rod-CeO_2 > Particle-CeO_2 > L-Particle-CeO_2 > Meso-CeO_2. The sharp peaks of B-Cube-CeO_2 and Commercial-CeO_2 exhibit high intensities, suggesting their large grain sizes and well-developed crystallinity. The weakest peak of Meso-CeO_2 indicates that with poor crystallinity, there exist lattice defects in the Meso-CeO_2 [19]. The existence of these lattice defects may affect the catalytic selectivity of azoxybenzene because it was confirmed to enhance the reduction of azoxybenzene to azobenzene according to reports [15].

To further explore the morphological characteristics, the surface areas of the series of CeO_2 catalysts were measured by the BET analysis and listed in Table 1. Surface areas of these catalysts exhibit a wide range of 5.48 m^2/g to 125.97 m^2/g. For most CeO_2 samples, a smaller crystallite size contributes to a larger surface area. However, both the crystallite size and surface area of Rod-CeO_2 are larger than that of L-Particle-CeO_2 and Particle-CeO_2, which is probably due to the agglomeration of crystallites during the synthesis processes of L-Particle-CeO_2 and Particle-CeO_2 [20]. For CeO_2 catalysts with different morphologies, the larger surface area commonly contributes to higher catalytic activities.

X-ray photoelectron spectroscopy (XPS) technique was carried out to investigate the surface atomic environment and the amounts of Ce valences for the seven CeO_2 catalysts. Fig. S3 (Supporting information) shows the Ce 3d core-level spectra of these CeO_2 catalysts. In accordance with spin-orbit doublets of $3d_{5/2}$ (V) and $3d_{3/2}$ (U), all the multiplets can be fitted with ten peaks, labeled as U' (901.9 eV), U^0 (898.6 eV), V' (883.9 eV), V^0 (880.6 eV), UV''' (916.1 eV), U'' (906.9 eV), U (900.3 eV), V''' (897.6 eV), V'' (888.5 eV) and V (881.9 eV) [21]. The main three $3d_{5/2}$ features (V, V'', V''') and the main three $3d_{3/2}$ features (U, U'', U''') are assigned to Ce^{4+} state. Moreover, Ce^{3+} state consists of all the satellites of $3d_{5/2}$ and $3d_{3/2}$ features, including V^0, V', U^0 and U'. Calculated by the relative integrated areas of Ce^{3+} and all the Ce 3d region, the amount of surface Ce^{3+} of CeO_2 samples are determined and listed in Table 1. The surface Ce^{3+} proportions follow the order Rod-CeO_2 > L-Particle-CeO_2 > Particle-CeO_2 > Meso-CeO_2 > S-Cube-CeO_2 > B-Cube-CeO_2 > Commercial-CeO_2. Considering the different redox ability of CeO_2 catalysts with various morphologies due to their different cyclic alternation ability between Ce^{3+} and Ce^{4+}, there possibly be a relationship of surface Ce^{3+} and catalytic activity for the series of CeO_2 catalysts.

The catalytic activities of the series of CeO_2 catalysts for reducing nitrobenzene to azoxybenzene were tested and listed in Table 1. It suggests that Ce^{3+} sites and surface areas of CeO_2 catalysts with various morphologies affect the conversion and selectivity of azoxybenzene respectively. From Table 1, appreciable reduction of nitrobenzene could be delivered by all catalysts described above, with azoxybenzene as the predominant product and azobenzene as the by-product. The Rod-CeO_2 exhibits the best catalytic performance, with the azoxybenzene yield which is 5.6 times higher than that of the Commercial-CeO_2. The catalysts of

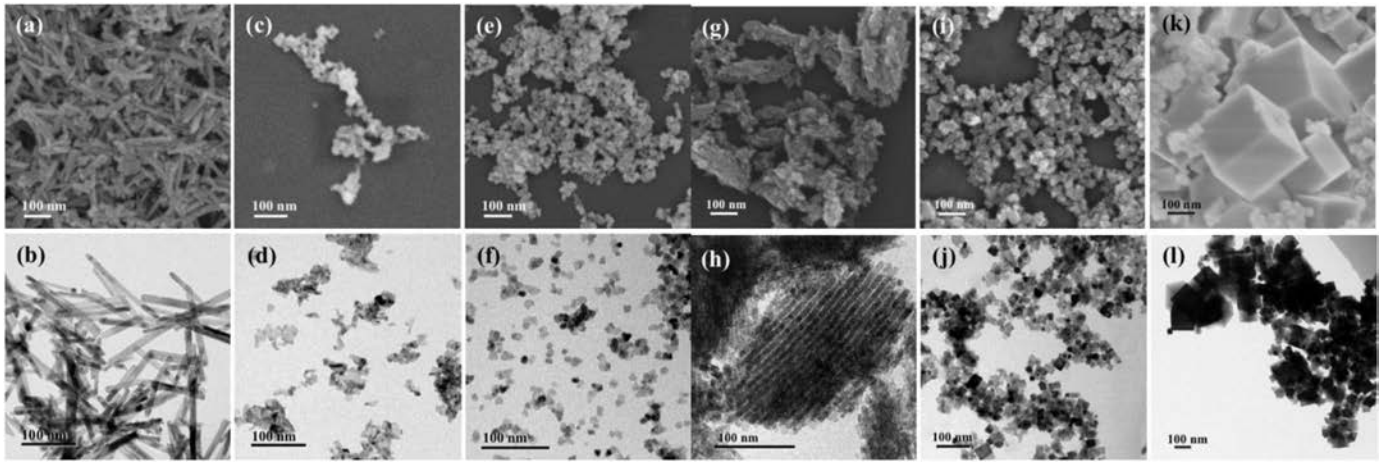

Fig. 1. SEM images of (a) Rod-CeO_2 (c) L-Particle-CeO_2 (e) Particle-CeO_2 (g) Meso-CeO_2 (i) S-Cube-CeO_2 (k) B-Cube-CeO_2, and TEM images of (b) Rod-CeO_2 (d) L-Particle-CeO_2 (f) Particle-CeO_2 (h) Meso-CeO_2 (j) S-Cube-CeO_2 (l) B-Cube-CeO_2.

Table 1
Summary of physico-chemical properties and catalytic performance of CeO_2 with various morphologies.[a]

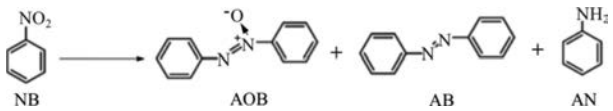

Entry	Shape	Size		SBET	Conv. [d]	$Ce^{3+}/(Ce^{3+}+Ce^{4+})$ [e]	Sel. [d] (%)		
		TEM [b]	XRD [c]	(m^2/g)	(%)	(%)	AOB	AB	AN
1	Rod	(9–18) × (70–320)	14.5	71.19	68.3	34.5	89.8	10.2	0
2	Long-Particle	5–20	11.1	65.48	65.0	31.78	85.7	14.3	0
3	Particle	5–18	12.4	63.19	59.4	31.09	85.8	14.2	0
4	Small-Cube	7–32	20.4	36.65	24.2	28.5	89.1	10.1	0
5	Big-Cube	16–140	74.2	5.48	13.2	24.96	100	0	0
6	Mesopore	—	10.0	125.97	30.7	29.1	77.1	22.9	0
7	Commercial	7–42	33.4	11.82	10.9	21.87	100	0	0

[a] Reaction conditions: nitrobenzene (1 mmol), CeO_2 (250 mg), CO (1 MPa), anhydrous toluene (5 mL), 150 °C, 6 h.
[b] Determined by TEM spectra.
[c] Determined by XRD.
[d] GC–MS analysis with oxylene as an internal standard.
[e] Determined by XPS.

entries 1–4 exhibit similar selectivity of azoxybenzene. The 100% selectivity of azoxybenzene by B-Cube-CeO_2 and Commercial-CeO_2 are in accordance with their relatively lower conversion. However, with 30.7% nitrobenzene conversion, Meso-CeO_2 shows only 77.1% selectivity of azoxybenzene with a large amount of azobenzene as the by-product. In many reports, the defects in catalysts could affect their catalytic performance [22,23]. According to the XRD and BET results, the existence of lattice defects in Meso-CeO_2 may result in the high activity of the by-product azobenzene. Moreover, compared with the catalytic activity which was tested under N_2 atmosphere and listed in Table S1 (Supporting information), the reductant CO is proved to improve the azoxybenzene yield, which is due to the role of CO on improving the redox ability of CeO_2 catalysts.

According to reports, there is a relative relationship between the support surface area of ceria-based Au catalysts and their catalytic performance for reducing nitrobenzene to azoxybenzene [15]. However, in this work, Meso-CeO_2 samples with the highest surface area exhibit only 23.7% yield of azoxybenzene, which indicates that surface area of ceria catalysts is not the most important factor for the reaction of reducing nitrobenzene to azoxybenzene. By inspection of Fig. 2, it is worth noting that the yields of azoxybenzene are highly dependent on the surface Ce^{3+} proportion for all CeO_2 catalysts, which suggests that surface Ce^{3+} proportion is the key parameter for azoxybenzene synthesis. Therefore, the improvement of surface Ce^{3+} proportion is of great importance to obtain a high yield of azoxybenzene.

To obtain the highest yield of azoxybenzene catalyzed by the Rod-CeO_2, the variation reaction was carried out and illustrated in Fig. 3 with the reaction condition (nitrobenzene (0.5 mmol), catalyst (250 mg), CO (1 MPa), anhydrous toluene (5 mL), 150 °C). The increasing trend with the reaction time could be observed in the conversion of nitrobenzene and the yield of azoxybenzene. After the 7 h reaction, the Rod-CeO_2 catalyst performed completely conversion of nitrobenzene and 89.8% azoxybenzene yield. Notably, only a certain amount of azobenzene as a by-product was formed during all the reactions.

To gain further insight into the reason of azoxybenzene with high selectivity as the main product, the preliminary mechanistic analysis was performed by monitoring the initial conversion rate of nitrobenzene along with azoxybenzene catalyzed by Rod-CeO_2. The corresponding rates were $r_1 = 0.185$ mmol $g^{-1} h^{-1}$ and

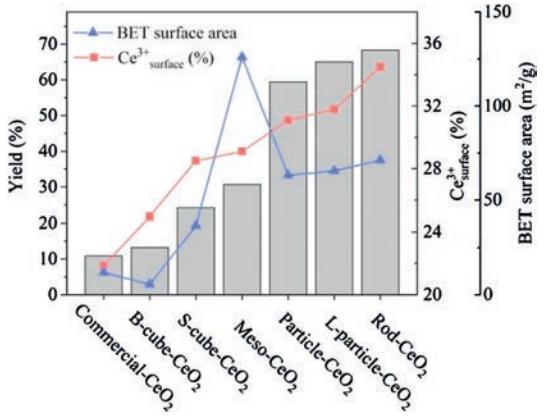

Fig. 2. Correlation between the Ce^{3+} proportion/BET surface area and catalytic performance of CeO_2 catalysts with various morphologies.

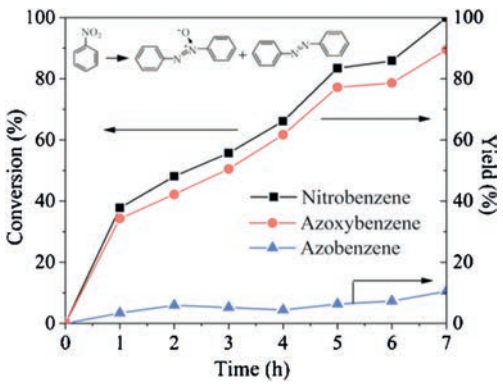

Fig. 3. Catalytic properties as a function of reaction time over the Rod-CeO_2 catalyst.

$r_2 = 0.075$ mmol $g^{-1} h^{-1}$ respectively (Scheme S1 in Supporting information). Taking the previous mechanistic observations of related reaction systems and our experimental analysis into consideration, a surface-redox reaction pathway on different active sites of ceria catalysts for azoxybenzene and by-product azobenzene production is proposed. The conversion of

nitrobenzene to azoxybenzene rely upon the presence of surface Ce^{3+} sites. Then azoxybenzene may undergo a further deoxygenation occurring on the lattice defects to produce the by-product azobenzene. This route is well supported by the above preliminary mechanistic results of Rod-CeO_2 catalyst. Compared with other ceria catalysts, Rod-CeO_2 exhibits the highest Ce^{3+} proportion but relatively lower surface area, which is related to the much higher conversion rate of nitrobenzene than that of azoxybenzene for Rod-CeO_2 and causes the inhabitation of azobenzene production.

In conclusion, the physico-chemical properties of the series of CeO_2 samples with different morphologies and their catalytic performance were explored in this work. The significant enhancement of azoxybenzene yield with the increasing Ce^{3+} proportion indicates that the surface Ce^{3+} proportion is the key ingredient for azoxybenzene synthesis. With the highest surface Ce^{3+} proportion, the Rod-CeO_2 exhibited completely conversion of nitrobenzene and 89.8% azoxybenzene selectivity in 7 h at 150 °C under 1 MPa CO. The preliminary mechanistic analysis clarified the high selectivity of azoxybenzene of Rod-CeO_2 by indicating the inhabitation of azoxybenzene to by-product azobenzene. Therefore, synthesizing surface-Ce^{3+}-richer CeO_2 catalysts is proposing for the green synthesis of azoxybenzene and further research.

Declaration of competing interest

The authors declare that they have no known competing financial interests or personal relationships that could have appeared to influence the work reported in this paper.

Acknowledgments

This work was supported by the National Natural Science Foundation of China (Nos. 51836006, U1609212), and Key Research and Development Project of Shandong Province (No. 2019JZZY010403).

Appendix A. Supplementary data

Supplementary material related to this article can be found, in the online version, at doi:https://doi.org/10.1016/j.cclet.2020.05.023.

References

[1] A. Grirrane, A. Corma, H. García, Science 322 (2008) 1661–1664.
[2] N.S. Allen, Colour Chemistry, 1st. ed., VCH Verlagsgesellschaft, Weinheim, 1987.
[3] S. Ghosh, S.S. Acharyya, T. Sasaki, et al., Green Chem. 17 (2015) 1867–1876.
[4] B. Paul, S. Vadivel, N. Yadav, S.S. Dhar, Catal. Commun. 124 (2019) 71–75.
[5] S. Sakaue, T. Tsubakino, Y. Nishiyama, Y. Ishii, J. Org. Chem. 58 (1993) 3633–3638.
[6] Y. Yang, S. Li, C. Xie, et al., Chin. Chem. Lett. 30 (2019) 203–206.
[7] T. Hou, Y. Wang, J. Zhang, et al., J. Catal. 353 (2017) 107–115.
[8] M.N. Pahalagedara, L.R. Pahalagedara, J. He, et al., J. Catal. 336 (2016) 41–48.
[9] L. Liu, P. Concepción, A. Corma, J. Catal. 369 (2019) 312–323.
[10] W. She, T. Qi, M. Cui, et al., ACS Appl. Mater. Interfaces 10 (2018) 14698–14707.
[11] H. Zhao, S. Yin, L. Lu, et al., J. Hazard. Mater. 381 (2019) 121037.
[12] Y. Men, J. Su, X. Wang, et al., Chin. Chem. Lett. 30 (2019) 634–637.
[13] Y. Yan, H. Li, Z. Lu, et al., Chin. Chem. Lett. 30 (2019) 1153–1156.
[14] Z. Wu, D.R. Mullins, L.F. Allard, Q. Zhang, L. Wang, Chin. Chem. Lett. 29 (2018) 795–799.
[15] H.Q. Li, X. Liu, Q. Zhang, et al., Chem. Commun. 51 (2015) 11217–11220.
[16] M. Lykaki, E. Pachatouridou, S.A.C. Carabineiro, et al., Appl. Catal. B: Environ. 230 (2018) 18–28.
[17] X. Zheng, Y. Li, L. Zhang, et al., Appl. Catal. B: Environ. 252 (2019) 98–110.
[18] X. Zhang, R. You, D. Li, T. Cao, W. Huang, ACS Appl. Mater. Interfaces 9 (2017) 35897–35907.
[19] S. Wang, L. Zhao, W. Wang, Y. Zhao, et al., Nanoscale 5 (2013) 5582–5588.
[20] H. Liu, W. Zou, X. Xu, et al., CO_2 Util. 17 (2017) 43–49.
[21] R. Peng, X. Sun, S. Li, et al., Chem. Eng. J. 306 (2016) 1234–1246.
[22] H. Zhao, G. Yang, X. Gao, et al., Environ. Sci. Technol. 50 (2016) 1056–1064.
[23] H. Zhao, C.I. Ezeh, et al., Appl. Catal. B: Environ. 263 (2020) 117829.